JOURNAL OF MATERIALS SCIENCE 21 (1986) 1775–1785

Isotactic polypropylene/EPDM blends: effect of testing temperature and rubber content on fracture

F. COPPOLA, R. GRECO, G. RAGOSTA
Institute of Research on Polymer Technology and Rheology, Arco Felice, Naples, Italy

Charpy impact tests in the temperature range −100 to +20° C have been carried out on two isotactic polypropylenes (PP) having different molecular weight and their blends containing as rubbery phase an ethylene–propylene–diene terpolymer (EPDM). For fractures of brittle nature the impact data were analysed in terms of the linear elastic fracture mechanics and K_c and G_c were determined. This behaviour was observed for the homopolymers over the temperature range investigated, and for the blends only up to −20° C. At higher temperatures such materials showed fracture of a semiductile type with visible evidence of craze whitening around the crack tip, followed by brittle type fracture. In this case the results were analysed in terms of a ductile contribution (energy required to form the crazed area) and of a brittle one (relative to the crack propagation area) from which G_c could be derived according to a procedure proposed in the literature. Tentative interpretations of the results also on a molecular and structural basis have been given. A critical discussion of the elaboration of the semiductile fracture data proposed in the literature has also been provided.

1. Introduction

In recent years there has been a considerable increase in the use of linear elastic fracture mechanics (LEFM) for studying the impact behaviour of thermoplastics, particularly in the case of glassy polymers [1, 2]. This is due mainly to the fact that results from a conventional impact testing are generally reported in terms of "impact strength" defined as the energy absorbed to break a notched specimen per unit area of fractured surface [3]. Such a means of analysis of impact data is not very satisfactory because this parameter is not a material property but is strongly dependent on the specimen geometry and type of test used [4]. To overcome these difficulties considerable efforts have been made by several researchers to obtain more useful fracture parameters from impact tests. In particular, Williams and co-workers [5–7] have shown that when fractures are of brittle nature the LEFM theory can be extended to the impact data. The use of such a theory permits the expression of the toughness of the material by two parameters which are material properties. One is the critical strain energy release rate (G_c) and the other is the critical stress intensity factor (K_c). Both these parameters describe accurately the conditions for the initiation of an unstable fracture process in brittle polymers. The fracture mechanism theory has also been extended to tougher polymers. This has been pursued by carrying out the experiments in suitable conditions: low temperatures and/or large specimens with very sharp notch, in order to reduce the amount of plastic zone at the crack tip. In fact some authors investigated non-crystalline polymers such as acrylonitrile–butadiene–styrene (ABS) [8, 9] and high-impact polystyrene (HIPS) [10, 11]. Recently, Fernando and Williams [12, 13] extended the LEFM theory to analyse the fracture behaviour of semicrystalline polymers such as polypropylene and ethylene–propylene copolymers. In this last case the fracture toughness, K_c, was evaluated over a wide range of temperature, thickness, notch sharpness and different modes of loading. Successively PP/EPR and PP/EPR/HDPE blends [14] were investigated to compare their behaviour with that of EP-copolymers. Very similar morphology and properties were found between copolymers and blends. In the present paper, a study of the impact fracture behaviour of two isotactic polypropylene (PP), having different molar mass and their blends containing as impact modifier an ethylene–propylene–diene terpolymer (EPDM), has been performed using the concepts of LEFM. The main purpose was to evaluate the dependence of G_c and K_c, under suitable testing conditions, on temperature, molecular characteristics of PP and blend composition. In addition, the influence of the morphology of the dispersed phase (EPDM) on the fracture toughness was also investigated. The behaviour of such materials at temperatures where they exhibit a semiductile fracture was also studied, to evaluate G_c and K_c relative to the fast crack propagation zone. The purpose of the last part of the work was also to evaluate the reliability of the approach proposed by some authors [8].

2. Experimental details

2.1. Materials

Two isotactic polypropylenes with different molar mass and molar mass distribution coded PP1 and PP2,

0022–2461/86 $03.00 + .12

TABLE I Characteristics of polymers used

Code	$\bar{M}_w$	$\bar{M}_n$	$\bar{M}_w/\bar{M}_n$	C_2(NMR-H) (mol %)	T_g (°C)	X_c (DSC) (%)	Company and trade name
PP1	6.3×10^5	1.9×10^5	3.3	–	−10 to 0	43	Exson Chemical Co. PP E_{111}
PP2	3.1×10^5	1.6×10^4	20	–	−10 to 0	50	RAPRA*
EPDM	3.1×10^5	1.2×10^5	2.5	80	−40	10	Exson Chemical Co. Vistalon 3708

*Rubber and Plastics Research Association of Great Britain.

respectively, and an ethylene–propylene–diene terpolymer (EPDM) were the materials used in this work. Some of their physical characteristics are given in Table I.

2.2. Blend and specimen preparation

Blends of the following PP/EPDM weight ratios: 100/0, 90/10, 85/15, 80/20, were obtained by melt mixing the homopolymers in a Brabender-like apparatus (Rheocord EC of Haake Inc.) at a temperature of 200° C with a residence time of 10 min and at a roller speed of 32 r.p.m. Compression-moulded sheets, 3.0 mm thick, were prepared by means of a heated press (Wabash Hydraulic Press) at 200° C and at a pressure of 240 kg cm^{-2}. Charpy-type specimens, 6.0 mm wide and 60 mm long were then cut by a mill.

All the specimens were notched at the middle point of their length as follows: first a blunt notch was made and then a very sharp notch 0.1 mm deep was produced by a razor blade fixed to a micrometric apparatus. The final value of notch depth was measured, after fracture, using an optical microscope.

2.3. Morphological analysis

An ultramicrotome LKB equipped with low-temperature cryokit and glass knives was used to obtain smooth surfaces for scanning electron microscopy (SEM) observations. For a better resolution of the morphology an etching technique based on the dissolution of the rubber phase was adopted. The microtomed surface were exposed to n-eptane boiling vapour for 30 sec and subsequently examined using a Philips 501 SEM after coating with gold–palladium alloy. Scanning electron micrographs showed that n-eptane selectively dissolved EPDM leaving PP undissolved.

2.4. Fractography

A morphological investigation of some fractured surfaces was performed by means of a Philips 501 SEM after coating the broken surfaces with Au/Pd, and by a Wild M 420 optical microscope.

2.5. Impact fracture measurement

Charpy impact tests were carried out at an impact speed of 1 m sec^{-1} using an Instrumented Pendulum (Ceast Autographic Pendulum MK2). For all the materials examined a set of specimens with various crack lengths and a span of 48 mm were broken at different temperatures ranging from −100 to 20° C. The temperature was changed by means of a liquid nitrogen home-made apparatus. Therefore, curves of energy and load against time or displacement were recorded for each test temperature.

3. LEFM analysis

3.1. Brittle behaviour

The critical stress intensity factor (K_c) was calculated using the equation:

$$K_c = Y\sigma_c a^{1/2} \quad (1)$$

where σ_c is the failure stress, a is the initial crack length and Y is a calibration factor depending on the specimen geometry. The values of Y used here are those given by Brown and Srawley [15]. On the grounds of Equation 1, a plot of $\sigma_c Y$ against $1/a^{1/2}$ gives a straight line with K_c as the slope. Graphs of this type were obtained from each material and K_c determined. An example of such an analysis is reported in Fig. 1 for PP1 homopolymer.

For calculation of G_c the following equation was used:

$$G_c = U/BwΦ \quad (2)$$

where U is the fracture energy, B and w are the specimen thickness and the width, respectively, and Φ is a calibration factor which is related to the specimen compliance (C) and the crack length by the following equation:

$$Φ = C/\mathrm{d}C/\mathrm{d}(a/w) \quad (3)$$

Values of Φ for Charpy tests have been tabulated for different geometries by Plati and Williams [5]. Equation 3 predicts that a graph of U against $BwΦ$ should give a straight line with G_c as the slope. Generally there is a positive energy intercept due to the fact that U contains a kinetic energy term (U_k) which must be subtracted in order to determine the energy stored in the specimen up to the crack propagation.

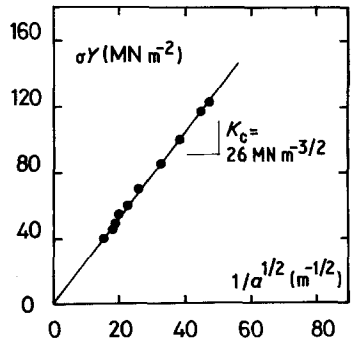

Figure 1 σY as a function of $1/a^{1/2}$ for PP1 homopolymer at −50° C.

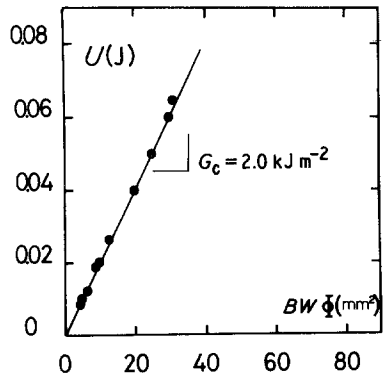

Figure 2 Impact fracture energy, U, as a function of $Bw\Phi$ for PP1 homopolymer at $-50°$ C.

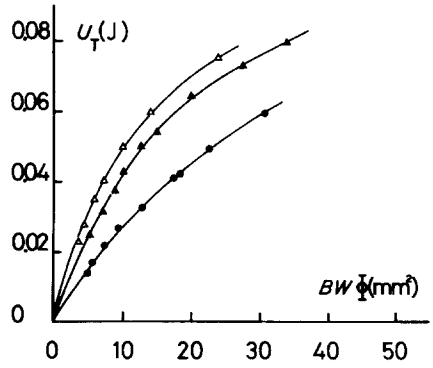

Figure 4 Total energy at break, U_t, as a function of $Bw\Phi$ for PP2/EPDM blends at 20° C. (●) blend 95/5; (▲) blend 90/10; (△) blend 85/15.

In this way Equation 3 becomes:

$$G_c = U - U_k/Bw\Phi \quad (4)$$

U_k was estimated separately by impacting an unsupported specimen. An example of G_c so determined is shown in Fig. 2 for PP1 homopolymer. The values of G_c obtained by energy measurements were also compared with those calculated using the equation:

$$G_c = K_c^2/E \quad \text{(plane stress condition)} \quad (5)$$

in which E is the Young's modulus. E values were determined by rebound tests [16] performed on unnotched specimens using the same instrumented pendulum at low impact speed ($\cong 0.1 \div 0.2$ m sec^{-1}).

3.2. Semiductile behaviour

Both PP1 and PP2 based blends show a semiductile fracture behaviour, in the ranges -20 to $0°$ C and -20 to $+20°$ C, respectively. In fact in Figs. 3 and 4 the total energy, U_t, at break against $Bw\Phi$ for all the blends containing up to 15% EPDM do not show a linear trend but a curvilinear one. Therefore, the LEFM is not directly applicable, since the plastic zone formed at the crack tip invalidates the model assumptions. However, after Williams [8] one can try to take into account the deviations from the ideality of the model by increasing the crack length by a certain amount, a_p, which is less or equal to the actual size of the plastic zone developed at the crack tip. In this way it is possible to estimate the plastic contribution to the total energy dissipation and to isolate by difference the amount of energy relative only to the brittle fracture behaviour (fast crack propagation). This procedure yields a G_c value to which at a first approximation, one could attribute an analogous meaning to that calculated in the previous paragraph.

To this purpose, a plot of U_t against the ligament area $B(w - a)$ is utilized (Fig. 5). From the slope of the extrapolated straight line passing through the origin one can calculate the energy per unit area needed for a crack opening in the case of complete ductile behaviour. Such a value multiplied by the crazed area, experimentally measured on the fracture surface by an optical microscope, gives the energy U_p relative to such an area.

From the plot of $U_1 = U_t - U_p$ against $Bw\Phi$ one can calculate G_c (see Figs. 6 and 7). It is to be noted that Φ, the geometrical factor, has been derived as a function of the total crack length $a_t = a + a_p$.

4. Results and discussion

4.1. Morphological characterization

Scanning electron micrographs of etched surfaces (by n-eptane boiling vapour) of PP1 and PP2 based blends are reported in Figs. 8 and 9. As can be seen the etching is able to dissolve selectively the rubber phase where the PP remain unaffected. Therefore, circular holes where EPDM originally resided, are evident. The dimensions of these holes are strongly dependent on the type of PP matrix, being less than 1 μm diameter for all the PP1/EPDM blends (see Fig. 8) and of the order of 2 to 5 μm for the PP2/EPDM blends. This can be attributed to the fact that PP1 has a melt viscosity higher than PP2 and closer to that of EPDM,

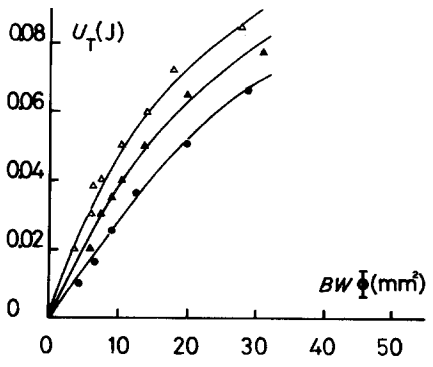

Figure 3 Total energy at break, U_t, as a function of $Bw\Phi$ for PP1/EPDM blends at 0° C. (●) blend 95/5; (▲) blend 90/10; (△) blend 85/15.

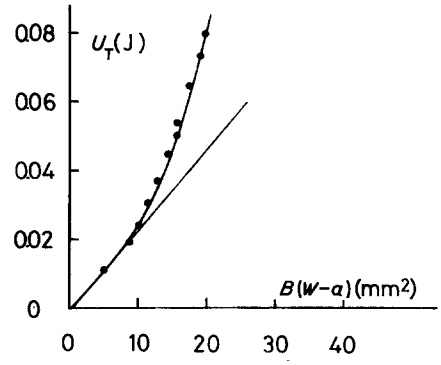

Figure 5 Total energy at break, U_t, as a function of $B(w - a)$ for PP2/EPDM (90/10) blend at $+20°$ C.

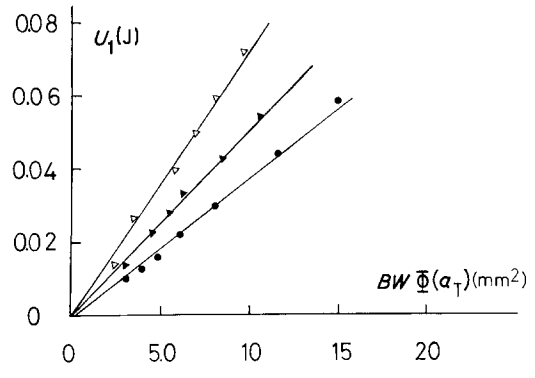

Figure 6 Corrected energy, U_1, as a function of $Bw\Phi(a_T)$ for PP1/EPDM blends. (●) blend 85/5; (▲) blend 90/10; (△) blend 85/15.

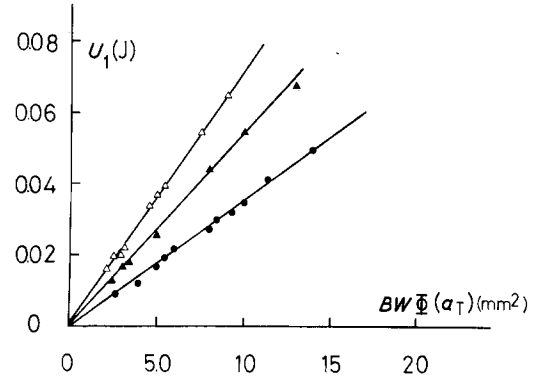

Figure 7 Corrected energy, U_1, as a function of $Bw\Phi(a_T)$ for PP2/EPDM blends. (●) blend 95/5; (▲) blend 90/10; (△) blend 85/15.

so that a finer size distribution of the minor component in the major one can be achieved. As reported subsequently, this difference in the domain sizes of the dispersed phase can play an important role in determining the fracture behaviour of such materials, especially at temperatures higher than $-20°$ C.

4.2. Fracture of the homopolymers

The shape of the recorded curves for PP1 and PP2 showed a linear behaviour up to fracture for all the temperatures and notch depths to width ratios investigated. The corresponding K_c and G_c values, calculated by the classical LEFM procedure (see Section 3.1), as a function of testing temperature are reported in Figs. 10 and 11, respectively. For both the homopolymers, K_c decreases slowly and linearly with enhancing the temperature. This dependence may be attributed to the lowering of the modulus which yields a lower strength. The increase in temperature, in fact, determines an increase of free volume in the material. Hence the crack starts to propagate in a softer body giving rise to a higher elongation to break but to a lower strength. This is confirmed by the G_c–T behaviour shown in Fig. 11 in which G_c appears to be

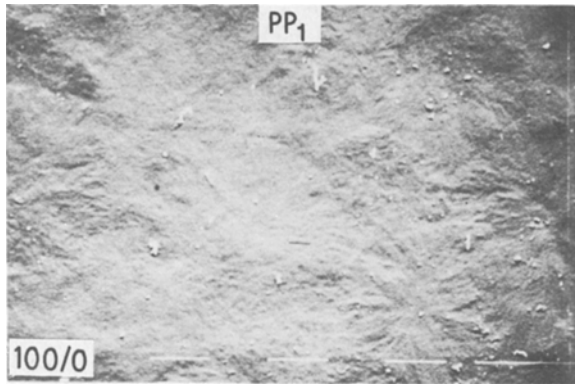

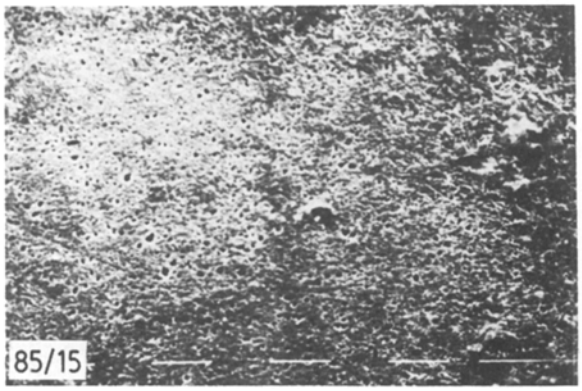

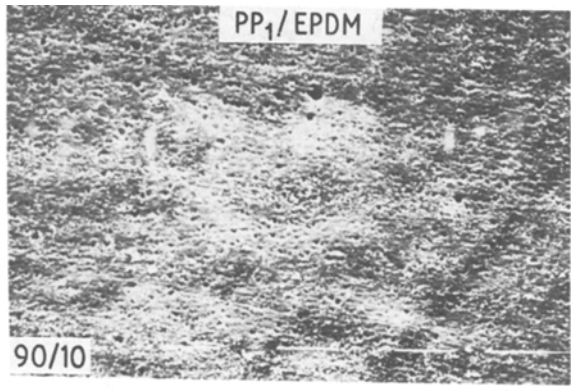

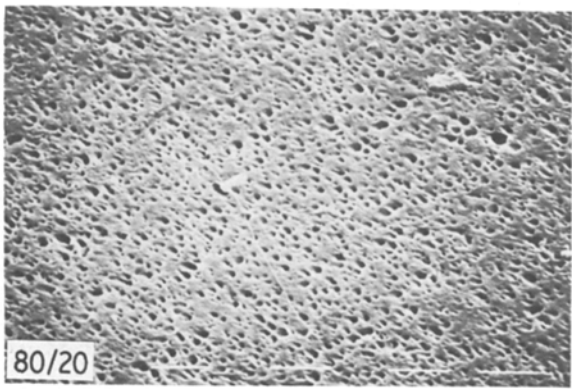

Figure 8 Scanning electron micrographs of etched surfaces of PP1 and PP1/EPDM blends. × 1250.

independent of temperature up to $-20°$ C for both polypropylenes. Since G_c is proportional to the energy to break, the product, F, times the displacement, s, must be constant. Therefore if s increases, F has to decrease. At temperatures higher than $-20°$ C, G_c starts to increase with an increasing slope. This trend can be attributed to the onset of the glass transition of the polypropylene. The surplus of energy with respect to the previous plateau value is necessary to overcome the consequent blunting of the notch. In other words the enhanced molecular mobility of the polymer chains determines a blunting of the notch and a new energy is required to recreate a sharp crack tip before the fracture propagation. This hypothesis is confirmed by the fractographic analysis shown in Fig. 12 where an induction area, visible on the left-hand side of the surface specimen fractured at $+20°$ C, is completely absent at $-100°$ C. As it is evident from both Figs. 10 and 11 the effect of varying the molecular weight of polypropylene, is that of a vertical shift of the curves. That is, the trend is completely the same, only the absolute values of K_c and G_c are increased with enhancing the molecular weight. This effect relies on the fact that a high polymer is an entangled system having a certain degree of pseudo crosslinking, with a viscoelastic plateau region which is longer the larger the molecular weight [17]. Hence at the same crystallization conditions the PP2 molecules (shorter in the average than the PP1 ones) will have a greater chance to disentangle from each other. Therefore, to cut a specimen into two pieces by fracture it is necessary to break PP chains, the more numerous the higher the molecular weight.

4.3. Fracture toughness of the blends

Different types of fracture were observed for PP/EPDM blends in the temperature range investigated.

1. Brittle behaviour. From -100 to $-20°$ C both PP1 and PP2 blends exhibited a brittle fracture behaviour and the LEFM analysis was suitable to describe the data.

2. Semiductile behaviour. At higher temperatures all the above mentioned blends showed fractures of a semiductile type with visible evidence of a cylindrical craze around the crack tip. In this case the impact data were tentatively analysed by attempting to take into account the energy dissipated by the crazed formation in evaluating the effective critical strain energy release rate. Furthermore, a diffuse triangular prism area, in addition to that localized around the tip, is present on the specimen for low notch depths (see Fig. 19).

3. Ductile behaviour. At temperatures higher than $0°$ C, for PP1/EPDM blends the fracture surface showed a completely ductile behaviour (see Fig. 21)

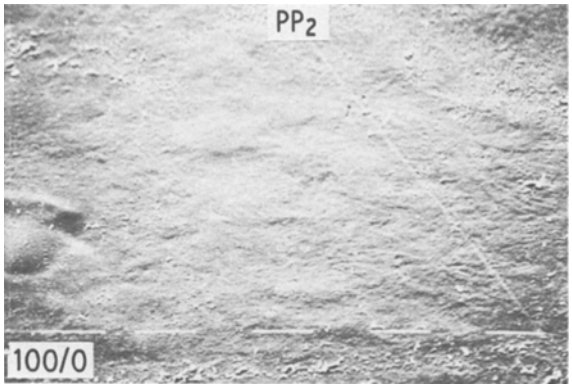

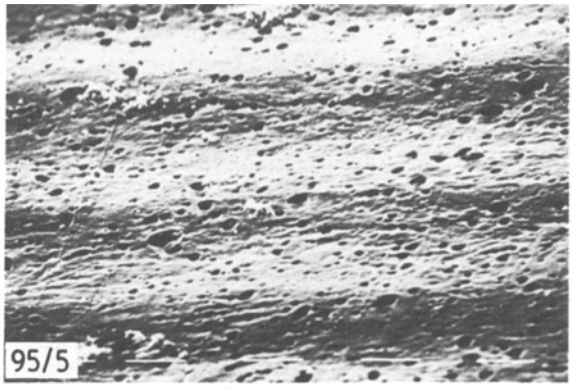

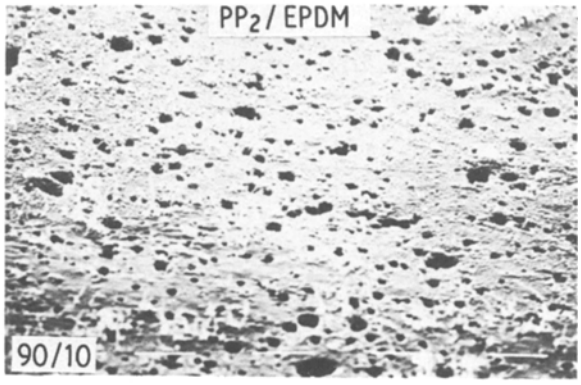

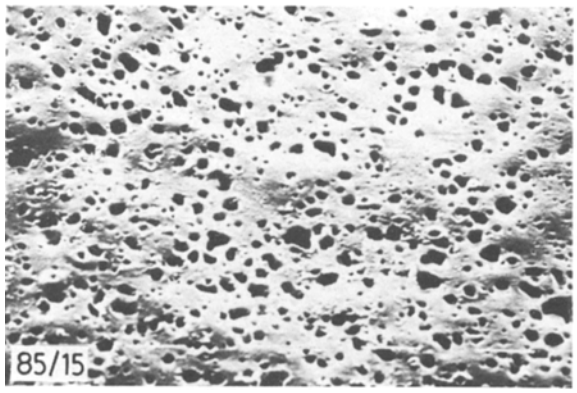

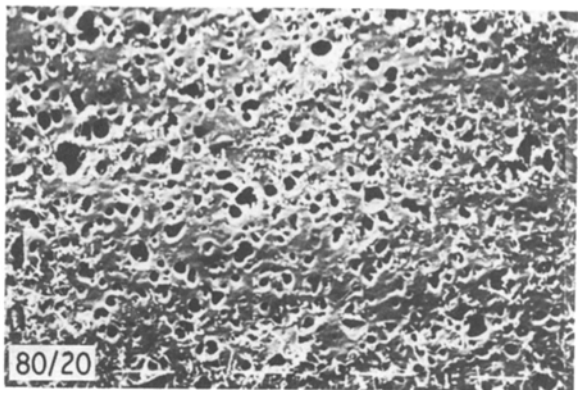

Figure 9 Scanning electron micrographs of etched surfaces of PP2 and PP2/EPDM blends. × 1250.

similar to that observed by Williams for ABS [8]. Also in this case, the triangular crazed area was observed at low values, as for PP2 blends.

4.3.1. Brittle behaviour

In Figs. 13 and 14, G_c as a function of temperature and of rubber content is reported for PP1/EPDM and PP2/EPDM blends, respectively. The G_c data relative to the homopolymers already previously discussed (Fig. 11) are shown for comparison as well. As it is possible to note, the latter show no dependence at all on temperature in the range -100 to $20°C$. On adding rubber, the observed straight lines increase their slope more and more with increasing rubber content. Analogously, in Figs. 15 and 16, K_c is reported for the same materials as indicated. For pure polymers there is a negative slope, whose value vanishes with increasing rubber content. In fact for the 80/20 blends there is almost no dependence of K_c on temperature.

From the two kinds of plots one can make the following considerations:

1. The blends show a G_c dependence and a K_c slight influence on the temperature whereas the opposite occurs for the homopolymers. This opposite behaviour can be attributed to the rubber particles lying along the notch tip. Their presence alters the tip radius yielding a sort of blunting effect (Fig. 17). This will require additional energy to create an effective sharp notch before the fast crack propagation yielding a G_c enhancement. The extent of the blunting will be the higher the greater the EPDM amount (more particles along the tip) and the temperature (lower modulus and therefore more deformation before fracture). K_c changes little with temperature and composition for the blends for the same reason. In fact the major effect is given by the particle size, which does not vary appreciably with increasing the EPDM content for the same PP matrix, as shown previously by the morphological observations (Figs. 8 and 9).

2. The increase in molecular weight brings an enhancement of G_c and K_c in the blends, as in the case of the homopolymers previously discussed (Figs. 11 and 12). However, the linear trends are little altered indicating a similar toughening mechanism induced by the EPDM particles in PP1 and PP2 based blends. Minor differences in behaviour can be observed in the synergism between the temperature and composition. In fact a 5% addition of EPDM yields a ΔG_c enhancement of about $0.9\,kJ\,m^{-2}$ for PP2 and of about $0.5\,kJ\,m^{-2}$ for PP1. The different value can be attributed to the higher notch blunting effect in the PP2 matrix of the EPDM particles, having larger dimensions than those imbedded in the PP1 matrix. Further rubber addition beyond 5% may have less influence on the more altered tip profile (PP2 matrix) than in the other case. These features are better shown in Figs. 18a and b where the same data of Figs. 13 and 14 have been replotted, respectively, in a different way. In Tables II and III, the G_c values obtained by energy measurement are compared with those calculated using Equation 5. As can be seen, the agreement is satisfactory with respect to the internal consistence of the data.

4.3.2. Semiductile and ductile behaviour

In Fig. 19 a photograph of PP2/EPDM (80/20) blend specimens, fractured at $+20°C$, is shown. Beside each sample the notch depths a on the left-hand side and the corresponding ligament area $B(w - a)$ on the right-hand side are reported. The relative impact energies as a function of the ligament area are shown for the same blend (solid line) and for others of lower EPDM content (dashed lines) in Fig. 20 as indicated. Starting from the bottom of Fig. 19, the first four samples exhibit laterally a circular stress whitening around the notch and part of fracture line. This corresponds in Fig. 20 to the first four points lying on the straight line OA passing through the origin O. On the successive three specimens two wings develop more and more with increasing ligament area (trait AB of the solid curve in Fig. 20). On the last four specimens the circular area is completely covered with a white triangle extended over most of the specimen (trait BC of the same curve). These features evidence for the 80/20 the strong dependence of the impact energy, U_t, on the notch depth, a. When this value is very small (cf. top of Fig. 19 the second specimen having $a = 0.1\,mm$ and very high impact energy $U = 0.2\,J$) the stress whitening is very extended and the total energy dissipated at the testing temperature, T, can be considered to be the sum of several contributions:

$$U_t = U_1S_1 + U_2S_2 + U_3v + U_4v' \qquad (6)$$

where: U_1S_1 is the energy dissipated to cut a fracture

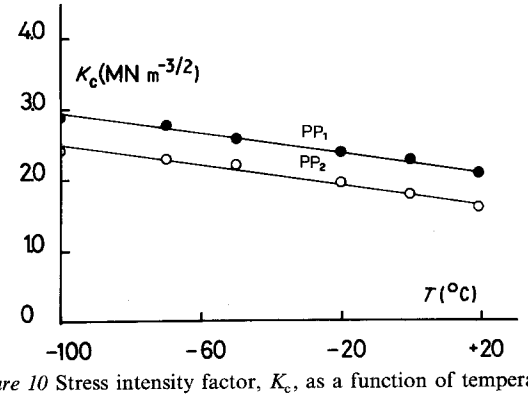

Figure 10 Stress intensity factor, K_c, as a function of temperature for PP1 and PP2 homopolymers.

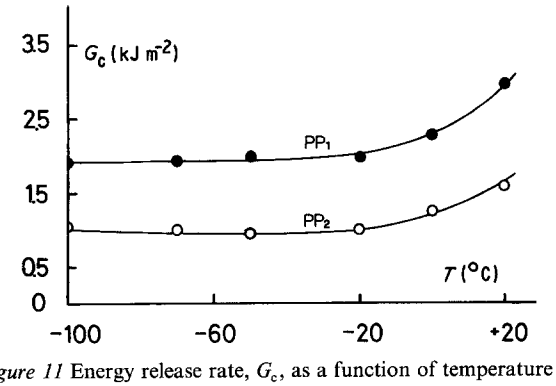

Figure 11 Energy release rate, G_c, as a function of temperature for PP1 and PP2 homopolymers.

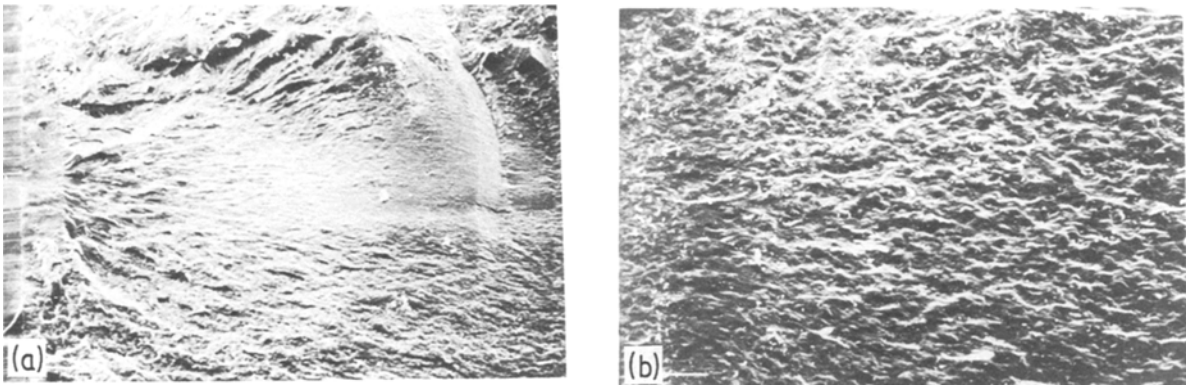

Figure 12 Scanning electron micrographs of fractured surfaces of PP2 homopolymer at (a) $-100°$ C and (b) 20° C. $\times 40$.

surface S_1 by fast crack propagation (brittle failure); U_2S_2 is the energy dissipated to cut a fracture surface S_2 by crazing (ductile failure); U_3v is the energy dissipated in a cylindrical volume, v, around the notch and the section S_2; U_4v' is the energy dissipated in a triangular prism volume, v', in addition to U_3v.

This analysis can also be applied to the lower EPDM content blends (85/15, 90/10, 95/5). In fact the A, B, and C levels indicate changes in the energy dissipation mechanism in all cases. The only difference consists in the fact that even for the 85/15 blend the EPDM amount, i.e. the particle concentration, is not sufficient to develop the triangular prism dissipation. But above the A level of energy the wings start to appear for all blends.

The phenomenon so far illustrated is quite different from that described by Williams for the ABS. For that material, in fact, a real ductile mechanism was developed just along the fracture surface. In other words the craze mechanism is strictly associated with the crack surface opening. In the case of PP2/EPDM, here discussed, the craze mechanism is instead dependent primarily on the EPDM phase dispersed in the PP2 matrix. Therefore, as soon as the stress concentration around the particles overcomes the yield stress of the matrix, a multiple craze effect appears. Naturally this occurs first at the crack tip giving rise to the cylindrical whitening discussed above. But at low notch depths this effect is also observed along the lines of greater tensile stress during the specimen bending, promoting first the wings appearing with decreasing a and eventually triangular prism whitening.

In the case of PP1 based blends, the crazing volume shape (see Fig. 21) is close to the ABS behaviour observed by Williams. This feature is due to the combination of a double effect of a more "cross-linked"

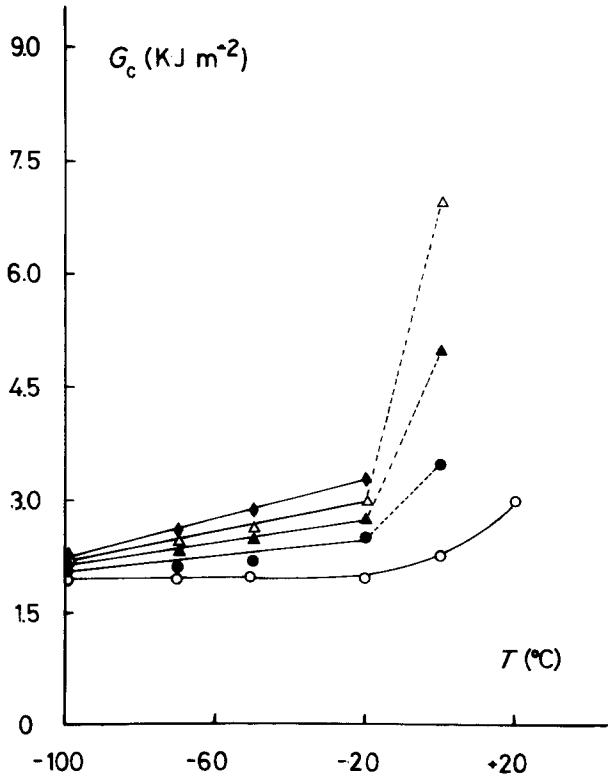

Figure 13 Energy release rate, G_c, as a function of temperature for PP1 and PP1/EPDM blends. (○) PP1; (●) blend 95/5; (▲) blend 90/10; (△) blend 85/15; (◇) blend 80/20.

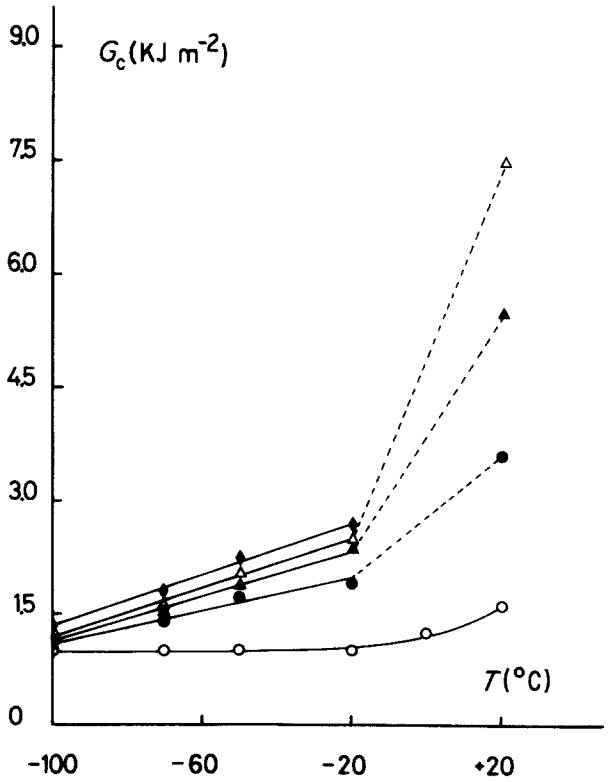

Figure 14 Energy release rate, G_c, as a function of temperature for PP2 and PP2/EPDM blends. (○) PP2; (●) blend 95/5; (▲) blend 90/10; (△) blend 85/15; (◇) blend 80/20.

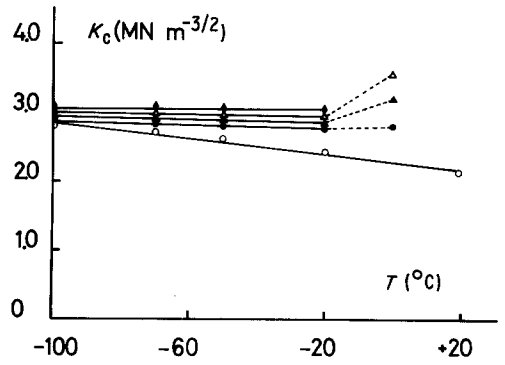

Figure 15 Stress intensity factor, K_c, as a function of temperature for PP1 and PP1/EPDM blends. (○) PP1; (●) blend 95/5; (▲) blend 90/10; (△) blend 85/15; (◇) blend 80/20.

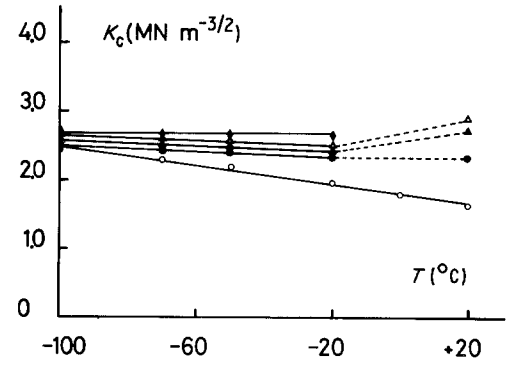

Figure 16 Stress intensity factor, K_c, as a function of temperature for PP2 and PP2/EPDM blends. (○) PP2; (●) blend 95/5; (▲) blend 90/10; (△) blend 85/15; (◇) blend 80/20.

matrix with smaller dispersed EPDM particles, yielding a more plastic behaviour. Only in this case, therefore, can one speak of a real ductile fracture which involves all the crack surface.

In the range from -20 to $+20°$ C the PP1 and PP2 based blends examined fail in a semiductile way, as previously mentioned. Two surfaces of specimens fractured at $+20$ and $-70°$ C of a 90/10 PP2 based blend are compared in Fig. 22. On the former an induction dark area underneath a crazed volume is clearly visible , which is absent in the latter. The G_c values, calculated according to the procedure described in Section 3.2, are shown in Figs. 13 and 14. The corresponding K_c values, determined by Equation 5 are reported in Figs. 15 and 16. In both cases G_c shows, beyond $-20°$ C, an upward trend, the higher the greater the EPDM content. Furthermore, for PP1 based blends, a sudden increase occurs at 0° C (at $+20°$ C the specimens do not undergo further fracture) and is displaced at $+20°$ C for PP2 based blends. With respect to K_c for PP1 and for 95/5 PP1/EPDM blends (Fig. 15), the same linear trend exists as in the lower temperature range -100 to $-20°$ C. At higher EPDM contents, K_c tends to increase from -20 to 0° C. On lowering the molecular weight a similar behaviour is observed. The more striking feature of the data illustrated above is that G_c seems to be too high with respect to the corresponding values at lower temperature. In fact, if the rupture mechanism in the fast crack propagation area is substantially the same,

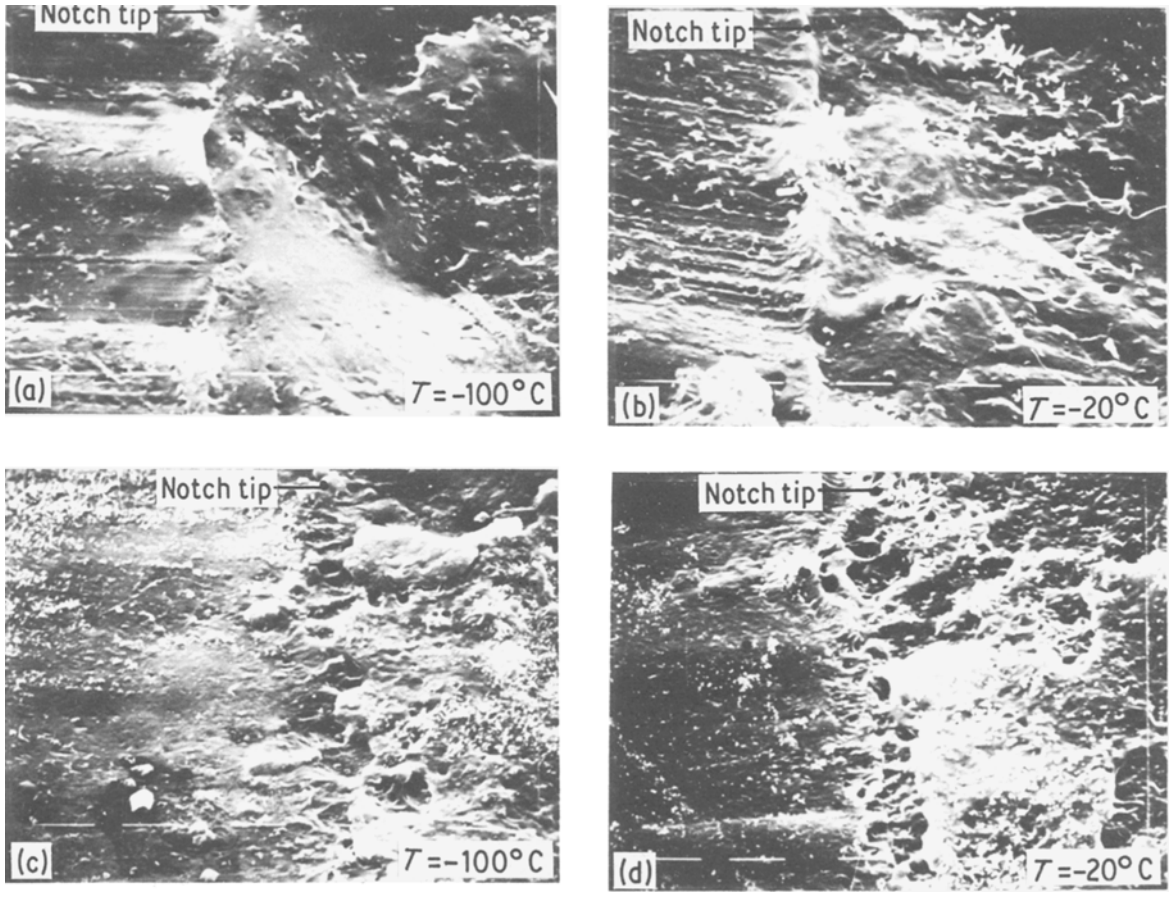

Figure 17 Scanning electron micrographs of fractured surfaces of (a, b) PP1 and (c, d) PP1/EPDM (80/20) blend. ×1250.

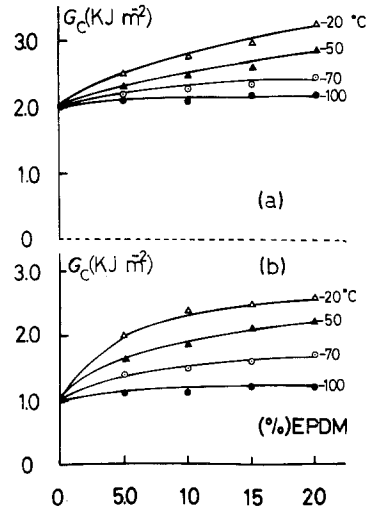

Figure 18 Energy release rate, G_c, as a function of EPDM content: (a) PP1/EPDM blends; (b) PP2/EPDM blends. Temperature as indicated.

the G_c values also should be comparable at all temperatures. But let us analyse the procedure followed to calculate G_c. For semiductile specimens Equation 6 becomes:

$$U_t = U_1 S_1 + U_2 S + U_2 v \quad (7)$$

since the energy contribution $U_4 v'$ relative to the triangular crazed volume prism, v', is not present.

Now let us assume that v is directly proportional to S_2

$$v = KS_2 \quad (8)$$

where K is a constant. Substituting Equation 8 into Equation 7 one obtains:

$$U = U_1 S_1 + (U_2 + k\mathrm{K}U_3) S_2 \quad (9)$$

For completely ductile specimens (small ligament areas), $S_1 = 0$; therefore by an extrapolation to vanishing S_2 values, one should calculate the energy ductile contribution:

$$U_p = (U_2 + KU_3) \quad (10)$$

Finally, U_1 can be estimated by difference.

Williams follows an analogous procedure for ABS even though it is not completely clear how his extrapolation has been performed in practice. Furthermore, from his U_t against v and U_t against S_2 plots one can derive the following relationship:

$$v = KS_2 + b \quad (11)$$

where b is a positive constant. Therefore $v = b$ for $S_2 = 0$.

From such a consideration one can understand that the separation procedure of the total energy, U_t, in ductile and brittle contributions is very crucial in determining meaningful G_c values from a physical point of view. But what can be even more important is the graphical G_c calculation from the plot of U_1 against BD. In fact the geometrical factor, Φ, is determined using corrected a values. The initial notch depth a is increased by an a_p increment, which is intended to be the ductile contribution. However, no real physical meaning can be attributed to a_p that becomes an adjustable parameter to straighten the U_1 against BDΦ curve. As it is possible to observe in Fig. 23, one can obtain different straight lines with a_p varying from zero up to the value equal to r_p, the observed crazed surface depth. The corresponding G_c values range from 3.8 to 7 kJ m^{-2}. Therefore it seems that no reliable G_c data can be obtained by this procedure. Our feelings would suggest that only a slight increase of G_c can be reasonable beyond $-20°$ C with respect to the lower temperature value, the

TABLE II G_c and E values at different temperatures for PP1 and PP1/EPDM blends

Materials	G_c(kJ m^{-2}) from energy data	$G_c = K_c^2/E$ (kJ m^{-2})	E (MN m^{-2})	T (°C)
PP1	1.9	2.0	4200	−100
	1.9	2.0	4000	−70
	2.0	1.8	3810	−50
	2.0	1.7	3350	−20
	2.3	2.3	2774	0
	3.0	2.9	1500	+20
95/5	2.1	2.1	4200	−100
	2.1	2.3	3690	−70
	2.2	2.3	3490	−50
	2.5	2.5	3014	−20
90/10	2.1	2.3	3920	−100
	2.3	2.4	3450	−70
	2.5	2.5	3360	−50
	2.8	2.9	2840	−20
85/15	2.2	2.3	3550	−100
	2.4	2.5	3300	−70
	2.7	2.8	3054	−50
	3.0	3.3	2500	−20
80/20	2.2	2.5	3352	−100
	2.5	2.8	3150	−70
	2.9	3.1	2900	−50
	3.3	3.6	2300	−20

TABLE III G_c and E values at different temperatures for PP2 and PP2/EPDM blends

Materials	G_c(kJ m^{-2}) from energy data	$G_c = K_c^2/E$ (kJ m^{-2})	E (MN m^{-2})	T (°C)
PP2	1.0	1.2	4620	−100
	1.0	1.18	4450	−70
	1.0	1.2	4100	−50
	1.0	1.1	3500	−20
	1.25	1.2	2800	0
95/5	1.1	1.3	4210	−100
	1.4	1.5	3800	−70
	1.7	1.5	3700	−50
	1.9	1.65	3200	−20
90/10	1.1	1.4	3930	−100
	1.5	1.6	3670	−70
	1.9	1.6	3550	−50
	2.4	2.1	2800	−20
85/15	1.2	1.5	3790	−100
	1.6	1.7	3300	−70
	2.1	2.0	2900	−50
80/20	1.30	1.7	3300	−100
	1.7	1.8	3100	−70
	2.2	2.2	2800	−50
	2.6	2.5	2500	−20

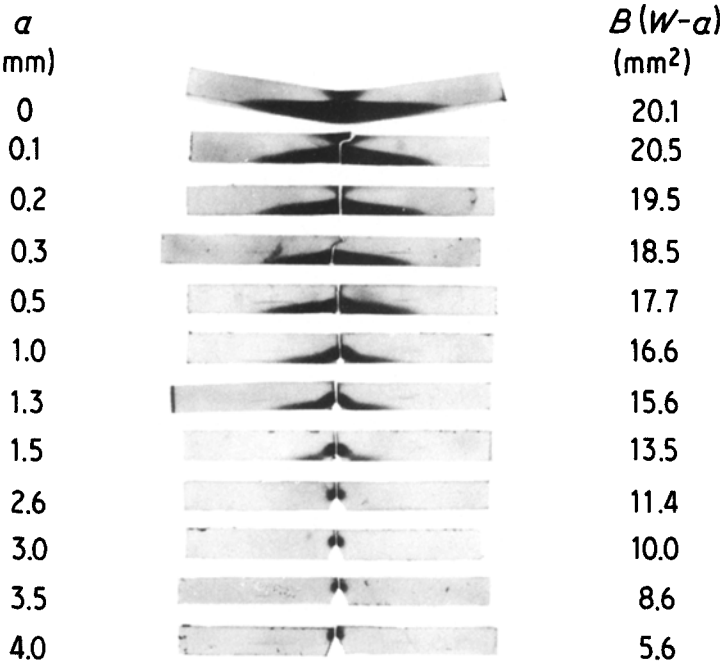

Figure 19 Photograph of fractured specimens of PP2/EPDM (80/20) blend; $T = 20°$ C.

remainder being due to erroneous calculations. In fact, in the case of PP1 and PP2 homopolymers, a limited augmentation of G_c can be observed, probably due to the onset of the glass transition temperature. This effect should still be valid for blends. In conclusion, the discussion of the semiductile behaviour, one can say that where brittle and ductile mechanisms are both acting in a fracture process, strong caution must be taken in the separation procedure to avoid misleading results.

5. Conclusions

The results of this work indicate that blends of isotactic polypropylene and ethylene–propylene–diene rubber show several fracture mechanisms which depend on the operating temperature, notch depth, matrix molecular characteristics and rubbery dispersed phase.

The enhancement of G_c and K_c in these blends with respect to the homopolymers is insufficient to render them high-impact technological materials. This is due to the low adhesivity of the particle rubbers to the matrix. Therefore, more complex formulation must be made to improve the impact resistance of the polypropylene at low temperatures and work is in progress in our Institute in this direction.

This study has been very useful from a scientific point of view in elucidating, in particular, the role of molecular weight of the matrix and that of the notch depth on the fracture behaviour of a semicrystalline matrix containing a free rubbery dispersed phase.

The LEFM is applicable over the whole temperature range for the homopolymers, whereas for the blends it is only up to $-20°$ C. At higher temperatures the procedure proposed in the literature by Williams overestimates G and K_c probably due to an incorrect separation of brittle and ductile contributions to the fracture.

Acknowledgement

This research was partially supported by a grant from the Progetto Finalizzato Chimica Fine e Secondaria of the National Research Council (CNR).

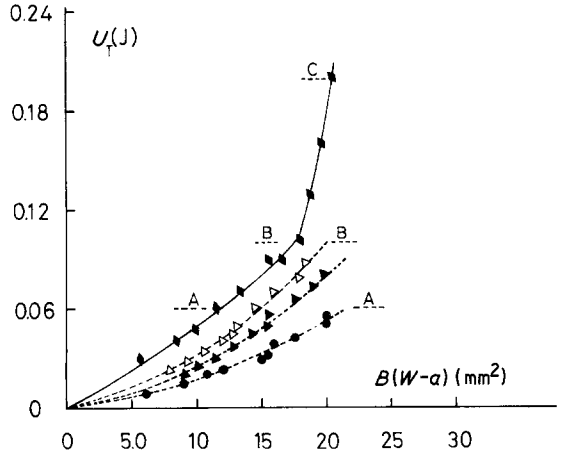

Figure 20 Total energy at break, U_t, as a function of $B(w - a)$ for PP2/EPDM blends at 20° C. (●) blend 95/5; (▲) blend 90/10; (△) blend 85/15; (◇) blend 80/20.

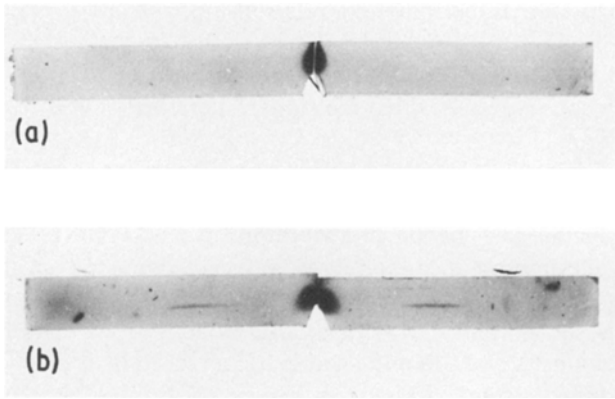

Figure 21 Photographs of fractured specimens of (a) PP1/EPDM (80/20) and (b) PP2/EPDM (80/20) blends.

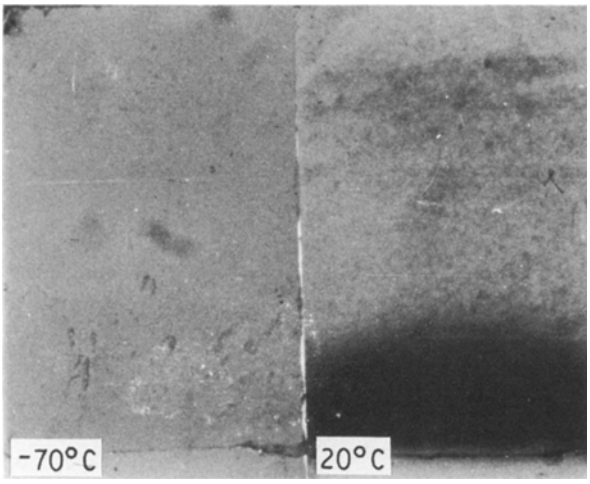

Figure 22 Optical micrograph of fractured surfaces of PP2/EPDM (90/10) blend at −70 and 20° C. ×15.

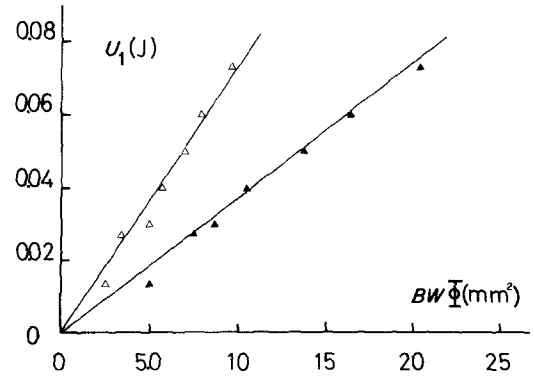

Figure 23 Corrected energy, U_1, as a function of $Bw\Phi$ for PP1/EPDM (85/15) blend. $a_p = 0$; a_p = crazed surface depth.

References

1. A. J. KINLOCH and R. J. YOUNG, "Fracture behaviour of polymers" (Applied Science, London, 1983).
2. G. P. MARSHALL, L. E. CULVER and J. G. WILLIAMS, *Plastics and Polymers* **75** February (1969) 75.
3. L. D'ORAZIO, R. GRECO, C. MANCARELLA, E. MARTUSCELLI, G. RAGOSTA and C. SILVESTRE, *Polym. Eng. Sci.* **9** (1982) 536.
4. P. I. VINCENT, "Impact test and service performance of thermoplastics" (Plastics Institute, London, 1971).
5. E. PLATI and J. G. WILLIAMS, *Polym. Eng. Sci.* **15** (1975) 470.
6. J. G. WILLIAMS, *ibid.* **17** (1977) 144.
7. L. V. NEWMANN and J. C. WILLIAMS, *ibid.* **20** (1980) 573.
8. *Idem, ibid.* **18** (1978) 893.
9. *Idem, J. Mater. Sci.* **15** (1980) 773.
10. K. NIKPUR and J. G. WILLIAMS, *ibid.* **14** (1970) 467.
11. *Idem, Plastics Rubber Mater. Appl.* **3** (1978) 163.
12. P. L. FERNANDO and J. G. WILLIAMS, *Polym. Eng. Sci.* **20** (1980) 215.
13. *Idem, ibid.* **21** (1981) 1003.
14. J. M. HODGKINSON, A. SAVADORI and J. G. WILLIAMS, *J. Mater. Sci.* **18** (1983) 2319.
15. W. F. BROWN and J. SRAWLEY, ASTM STP 410 (American Society for Testing and Materials, Philadelphia, Pennsylvania, 1966).
16. T. CASIRAGHI and A. SAVADORI, *Plastics Rubber Mater. Appl.* February (1980) 1.
17. J. D. FERRY, "Viscoelastic properties of polymers" (Wiley, New York, 1969).

Received 20 March
and accepted 11 July 1985